Multicarrier Multipactor Analysis Based on Branching Levy Walk Hypothesis

**Qingqing Song[1], Xinbo Wang[2, 3], Wanzhao Cui[2], Zhiyu Wang[1, *],
Yichen Shen[4], and Lixin Ran[1]**

Abstract—In this paper, we propose a stochastic approach for the analytical analysis of the multicarrier multipactor discharge occurring in high-power vacuum microwave devices, in which electric fields are not homogeneously distributed. We indicate that the statistical behavior of large amount of secondary electrons in the process of a multipactor discharge can be well described by the probabilistic random walk and Levy walk theory. Based on the derived probability density of the lateral diffusion of secondary electrons in homogeneous fields, the multicarrier multipaction in inhomogeneous fields can be analytically computed with significantly enhanced efficiency. As a demonstration, the accumulation of secondary electrons of a multicarrier multipaction in a rectangular waveguide supporting TE_{10} mode is given. The theoretical results comply well with the results achieved by the time-consuming particle simulation, the slope difference of which is less than 0.8%, while only costs one-order less computational time. To the best of our knowledge, this is the first time that the probability density of the lateral diffusion of secondary electrons during a multipaction is theoretically derived. This density depicts the physical picture of the statistical movement of secondary electrons during the process of a multicarrier multipactor, which can be widely used in the areas of high-power electronics and electromagnetism.

1. INTRODUCTION

It has been well recognized that when electrons in a vacuum cavity of microwave device are accelerated by high-power electric fields, their impingements against the metallic surface of the cavity may result in a self-sustained electron avalanche, i.e., multipactor discharge [1–5]. Recently, a new mechanism of multipactor discharge was found in wideband high-power systems when multiple carriers were used. In such a "multicarrier multipactor" [6–9], the fluctuation of secondary electrons between consecutive periods of the multicarrier signal can be accumulated, yielding a dynamic, "long-term" multipactor process [10, 11]. This special multipactor discharge can be induced by low-energy electric field, and therefore potentially threatens the reliability of the wideband high-power RF and microwave systems in space and accelerator applications.

Previously reported theoretical calculations of multicarrier multipactor can only be performed in homogeneous fields, wherein the lateral diffusion of secondary electrons is isotropic in all lateral directions [11]. In this case, it is not necessary to take the lateral diffusion into account. However, the real world is that the field distribution in almost all actual radio frequency and microwave devices is inhomogeneous, wherein the electrons' lateral diffusion is no longer isotropic and has to be considered in the calculation. In this paper, based on the approach provided in [11] that can be used to analyze the multicarrier multipactor under circumstances of homogeneous field distribution, we extend our prior
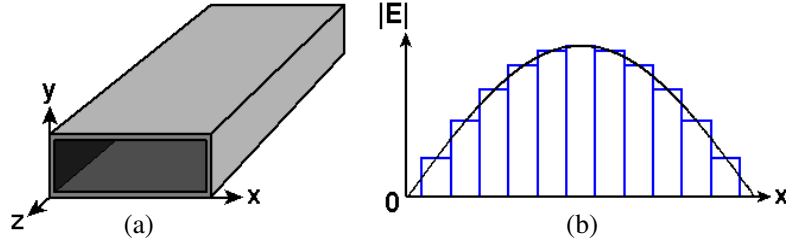
Figure 1. Discrete approximation of an inhomogeneous field distribution for multicarrier multipactor analysis.

research on the lateral diffusion of secondary electrons in the process of a multipactor, also for the homogeneous field distribution [12], to further demonstrate how the multicarrier multipactor under circumstances of inhomogeneous field distribution can be analytically computed. Without losing any generality, a metallic rectangular waveguide supporting a TE_{10} mode is chosen for this demonstration.

2. BRANCHING LEVY WALK HYPOTHESIS FOR MULTIPACTOR

Figure 1(a) shows a rectangular waveguide with dimensions defined in an x-y-z coordinates, carrying a half-sine electric field distribution of the TE_{10} mode depicted in Fig. 1(b). It is seen that in the x-y cross section, the electric field is no longer homogeneously distributed along the y direction, and therefore the approach proposed in [11] does not apply to this situation.

To compute the multicarrier multipactor in such a waveguide, its cross section can be divided into multiple regions, as shown in Fig. 1(b). When the number of such regions is sufficiently large, the field distribution in each region can be considered to be homogeneous, and the secondary electron yield (SEY) accumulated in each region during the process of multicarrier multipactor can thus be calculated based on [11]. However, before summing up all the SEYs of each region, the lateral diffusion of secondary electrons between different regions has to be known, such that the exchange of secondary electrons between such regions can be calculated.

We know that all analyses to the multipactor discharge are based on an SEY model and the probability densities of the release velocity and angle of secondary electrons [10]. When the field distribution is uniform, such as the field in a parallel plate waveguide, the lateral diffusion of the secondary electrons is statistically isotropic at each place, and therefore only one-dimensional motion of electrons along the direction of electric field needs to be considered. In this paper, we derive the probability density of the above lateral diffusion of a single electron in homogeneous fields based on the random walk and Levy walk hypotheses. Different from the analysis of conventional Brownian motion, where the random walk of a particle comes from its randomized collisions with a large amount of other particles, the random walk of a secondary electron comes from its large amount impingements against the metallic surfaces.

Figure 2 illustrates the top-view (left) and side-view (right) demonstrations of the lateral diffusions between two parallel metallic surfaces with homogeneous electric field polarized along the y direction. In the top-view demonstrations of Figs. 2(a) and 2(b), the SEYs are assumed to be 1 and 1.28, meaning that after 9 impingements, the total SEY statistically changes to 1 and 11, respectively. It is seen that the random movements of secondary electrons are similar to the Brownian motion. According to the probability theory, the stochastic behavior of the secondary electrons can be analyzed by the random branching Levy walk approach [13–18].

For simplicity, we firstly analyze the case when SEY = 1, where the branching Levy walk process reduces to the random walk process. According to [10], after each impingement, the release angle θ of a secondary electron included by the release velocity and the normal of the surface satisfies the probability density $p(\theta) = \sin 2\theta$. Meanwhile, the corresponding azimuth angle φ satisfies $p(\varphi) = 1/2\pi$. In Fig. 2, the movement of a secondary electron between the parallel surfaces consists of a series of random paths, each with a randomized reflection angle determined by $p(\theta)$ and $p(\varphi)$. Due to the fact that both $p(\theta)$ and $p(\varphi)$ are irrelevant to the accelerating electric field, the random walk can be
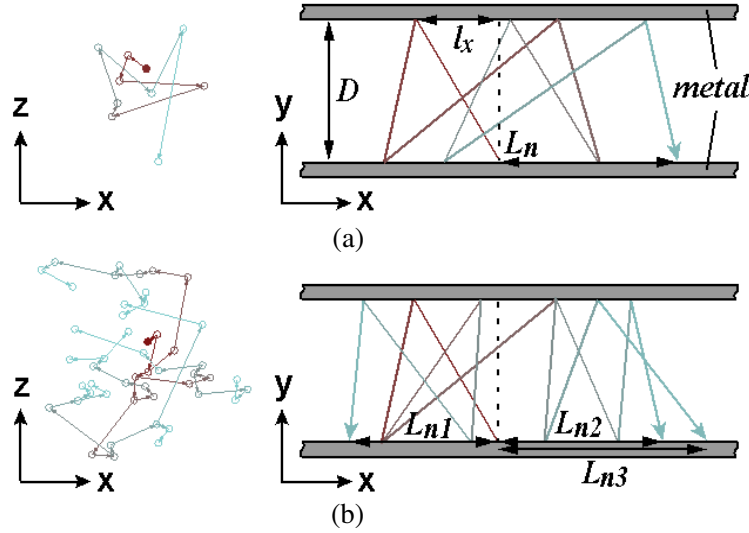
Figure 2. Lateral diffusion of secondary electrons perpendicular to a homogeneous electric field. Top-view (left) and side-view (right) demonstrates of the lateral diffusions of (a) random walk and (b) Levy walk.

regarded to be irrelevant to the accelerating field as well [10]. Theoretically, the transition time of a secondary electron between the parallel surfaces is determined by the release velocity, which satisfies the Maxwellian distribution [10], and the acceleration (or deceleration) by the electric field. However, since the randomized impingements to the surface are completely asynchronous with the periodic electric field, for a large amount of impingements, the effects to the lateral diffusion due to the accelerating field statistically cancels out.

In the following, we derive the probability density of the diffusion of the electrons along a specified lateral direction, i.e., the x direction. Assume such a diffusion satisfies a probability density $p(l_x)$, where l_x is the x-component of the lateral diffusion of a secondary electron after each impingement, as shown in Fig. 2(b). If the i-th impingement results in an x-component lateral displacement $l_{x,i}$, the total lateral displacement of the electron along the x direction after n impingements is

$$L_n = \sum_{i=1}^{n} l_{x,i} \tag{1}$$

Since $p(\theta) = \sin 2\theta$ and $p(\varphi) = 1/2\pi$, l_x after each impingement can always be expressed by $l_x = D \tan\theta \cos\varphi$. Consequently, at a fixed φ, we can obtain $dl_x = D \cos\varphi \cos^{-2}\theta d\theta$ and $d\theta = 1/(D\cos\varphi) \cos^2\theta l_x$. Since $p(\theta) = \sin 2\theta$ and $\int p(l_x,\varphi)dl_x = \int p(\theta)d\theta$, we have

$$p(l_x, \varphi) = 2\sin\theta\cos^3\theta/D\cos\varphi \tag{2}$$

Finally,

$$\lim_{l_x \to \infty} p(l_x) = 2\int_{\varphi=0}^{\pi/2} p(l_x,\varphi)p(\varphi)d\varphi = l_x^{-3}\frac{2D^2}{\pi}\int_{\varphi=0}^{\pi/2}\cos^2\varphi d\varphi \propto l_x^{-3} \tag{3}$$

It is seen that when $l_x \to \infty$, $p(l_x) \to l_x^{-(\mu+1)}$, where $\mu = 2$. In this case, the total lateral diffusion projected onto the x direction, i.e., L_n, satisfies an anomalous Gaussian distribution with its variance $\sigma^2 = n\ln n$ according to the central limit theory [13]. Thus we have

$$p(L_n) = \alpha e^{-L_n^2/2\beta n\ln n} \tag{4}$$

where α and β are constant normalization and calibration factors, respectively, and β is determined by the exact distribution of $p(l_x)$. It is seen that although the release angle of electrons obeys a non-uniform distribution, the lateral diffusion along the x direction obeys a special Gaussian distribution.
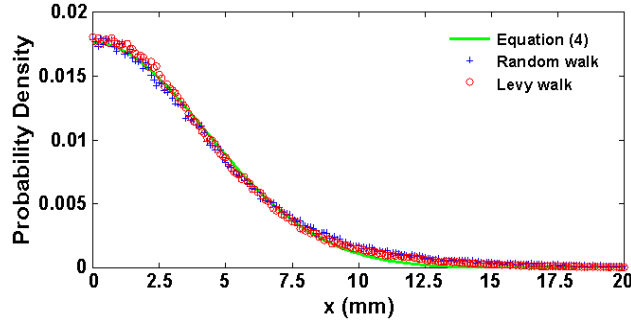
Figure 3. Verification based on simulated random walk and Levy walk.

When the SEY is not 1, the aforementioned lateral diffusion should be derived by the branching Levy walk analysis [18]. We will see later that under the circumstance of multipactor discharge, the form of the probability density remains unchanged.

To verify the obtained $p(L_n)$, using the same configuration as shown in Fig. 1, we run numerical simulations for a random walk with SEY = 1 and a Levy walk with SEY = 1.28 of a secondary electron that experiences 40 impingements, respectively. Such a simulation is repeated for 400000 and 40 times, respectively, and the probability density is then achieved by a statistical analysis to the simulation data. Note that for the Levy walk with SEY = 1.28, 40 impingements will yield a sufficiently large amount of secondary electrons. Fig. 3 plots the probability densities calculated by (4) (solid green line) with $\alpha = 17.6e-3$, $\beta = 0.66$, and the corresponding numerical analysis of random walk (blue cross) and Levy walk (red circles) processes. It is seen that the probability density of the Levy walk almost overlaps the random walk, and the theoretical curve fits well with both simulation curves. Due to the fact that the 1.28-SEY has been very large to ensure the occurrence of multipactor, we can conclude that in the attempt of calculating the threshold of a multipactor discharge, Equation (4) applies for all SEYs. Note that in almost all SEY models, the largest possible SEY is around 2 [4].

3. MULTICARRIER MULTIPACTOR IN A RECTANGULAR WAVEGUIDE

Assisted with Equation (4), we resume demonstrating the analytical computation of the multicarrier multipactor in the rectangular waveguide. To verify our result, we also perform a particle-in-cell (PIC) simulation using a commercial software packet, i.e., CST Particle Studio$^{\text{TM}}$, to the same rectangular waveguide. In both the calculation and simulation, the width of the waveguide is 58.17 mm, which is chosen to be the same with the standard waveguide WR229, the height is 0.43 mm, and the length of the waveguide is 100 mm. The height is chosen to be very small, such that it is more likely to make the multipactor discharge take place. With aforementioned dimensions, only TE$_{10}$ mode can be excited in the frequency range between 2.58 and 5.16 GHz. For the convenience to compare our result with previous literature, we choose the six-carrier signal used in [11] as the excitation. The frequencies of each carrier are 3.57, 3.67, 3.77, 3.87, 3.97 and 4.07 GHz, respectively, each with the same amplitude of electric field, i.e., 70000 V/m. Finally, we assume the surface of the inner cavity is coated with silver, and the same Furman SEY model [19] with the standard silver boundary is used in both calculation and simulation.

During the analytical computation, we equally discretize the half-sine distributed field of TE$_{10}$-mode into 11 rectangular regions, as shown in Fig. 1(b). In each region, the time evolution of accumulated secondary electrons is calculated following the statistical multipactor theory proposed in [11, 12], which is based on the transit time probability density (TTPD) $G(\tau|\varphi_s)$. $G(\tau|\varphi_s)$ is defined as the probability density for an electron released from a surface at phase $\varphi_s \in [0, 2\pi]$ and impacts a surface again at phase φ after the transit phase $\tau = \varphi - \varphi_s$ [11, 12]. Once obtained the TTPD functions, the accumulation of the secondary electrons can be obtained based on the non-stationary approach [11, 12], i.e.,

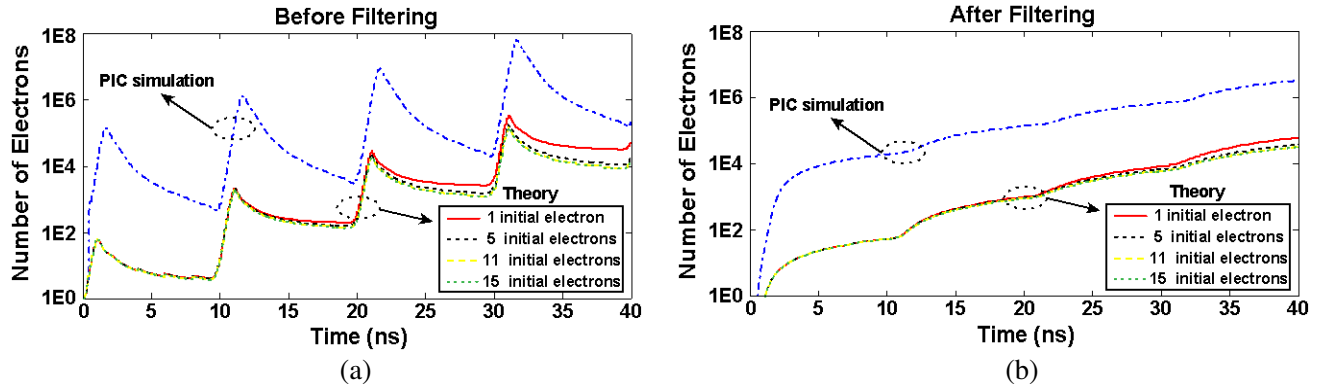$$N(\varphi) = \int_0^\varphi [C(\varphi) - I(\varphi)]d\varphi \tag{5}$$

Figure 4. The simulation and the theoretical results of the accumulation of electrons (a) before and (b) after a low-pass filtering.

where the relationship between the impact rate $I(\varphi)$ and the emission rate $C(\varphi)$ can be given by

$$I(\varphi) = \int_0^\varphi C(\varphi')G\left(\varphi - \varphi'|\varphi'\right) d\varphi' \tag{6}$$

To accelerate the calculation, we uniformly divide each period of the multicarrier signal into 20 segments. During the calculation, at the end of each segment, the exchange of accumulated electrons between adjacent regions is perform based on the probability density provided by Equation (4), and the total distribution of electrons in the cross section will be updated by a summation of the electrons in all regions.

To investigate the impact of initial electrons on the analytical analysis, we also assumed different initial electrons of 1, 5, 11 and 15, uniformly located in each region along the x direction. The analytically computed and the simulated electrons' accumulation are presented in Fig. 4(a), where the blue dash-dot curve represents simulated result and the other curves refer to the theoretical calculation results with 1, 5, 11, 15 initial electrons in each region, respectively. For the convenience to compare the overall accumulation trends of simulated and theoretical results, we also perform a low-pass filtering to the curves in Fig. 4(a), and the corresponding results are shown in Fig. 4(b), respectively.

In Fig. 4, the electron accumulations obtained by the particle simulation and the analytical computation have similar trends. Specifically, when the initial electrons are larger than 10, the theoretical accumulation curves begin to converge, and the overall accumulation rate of secondary electrons becomes almost the same as the simulated slope when the amount of accumulated electrons is sufficiently large. In Fig. 4(b), the slope difference between the simulated curve and the theoretical curve with 15 initial electrons is less than 0.8%, which is calculated from the linear fitting of the log-scale data after 20 ns. Note that the accumulation trend determines the occurrence of a multicarrier multipactor, and therefore the difference of the total number of electrons caused by different initial electron configurations between the calculation and simulation is not important. This result clearly validates the probability density of the lateral diffusion derived in Equation (4). However, it also indicates that the number of initial electrons influences the analytical result. We conclude this impact due to the less partitions used in the calculation. With 11 regions, although the field in each region can be considered to be homogeneous, the size of the region is too large compared with the scale of electrons' lateral diffusion. With increased initial electrons, the regions used to exchange electrons are equivalently increased, and the accuracy of the overall lateral diffusion in the cross section is accordingly enhanced. Comparing with the result obtained in [11], the electron population growing in our result is slower. This clearly indicates the effect of the lateral diffusion of electrons in the multicarrier multipactor under the circumstance of inhomogeneous field distribution.

The results achieved in Fig. 4 prove that our approach can be effectively used for multicarrier multipactor analysis under circumstances of inhomogeneous field distribution. Although we only demonstrate our method with a rectangular waveguide, it can apparently be used in any waveguides and microwave components with given electromagnetic modes. With the same computational capacity, our method only costs 1/8 of the time used by PIC simulation.

4. CONCLUSION

In conclusion, based on the random walk and branching Levy walk hypothesis, we provided a stochastic approach for the analytical analysis of multicarrier multipactor discharge for microwave components with inhomogeneous field distribution. By deriving the statistical depiction of the lateral diffusion of secondary electrons in the process of a multipactor in a homogeneously distributed field, we demonstrate how the multicarrier multipactor discharge in inhomogeneous field can be analytically computed. A metallic rectangular waveguide supporting a TE10 mode is chosen for the demonstration. Particle simulations are also conducted for validation. The theoretical analysis matches well with simulation result, the slope difference of which is less than 0.8%, while costs one-order less computational time. Although we only demonstrated an example using TE_{10}-mode rectangular waveguide, our method applies for all radio frequency and microwave devices with known transverse field distribution, which provides a useful tool for rapid analysis of multicarrier multipactor in practical applications. To the best of our knowledge, this is the first time that the probability density of the lateral diffusion of secondary electrons during a multipaction is theoretically derived. We pointed out that the lateral diffusion of an electron after N collisions satisfies a Gaussian distribution with a special standard variance. This probability density depicts the physical picture of the statistic movement of secondary electrons during a multipactor process, which can be used in a wide range of applications in the areas of high-power electronics and electromagnetism.

REFERENCES

1. Farnsworth, P. T., "Television by electron image scanning," *Journal of the Franklin Institute*, Vol. 218, 411, 1934.
2. Vaughan, J. R. M., "Multipactor," *IEEE Trans. Electron. Dev.*, Vol. 35, 1172, 1988.
3. Kishek, R. A., Y. Y. Lau, L. K. Ang, A. Valfells, and R. M. Gilgenbach, "Multipactor discharge on metals and dielectrics: Historical review and recent theories," *Phys. Plasmas*, Vol. 5, 2120, 1998.
4. ECSS, "Space engineering: Multipacting design and test," ESA Publication Division, Noordwijk, 2003.
5. Gill, E. W. B. and A. von Engel, "Starting potentials of high-frequency gas discharges at low pressure," *Proc. R. Soc. London, Ser. A*, Vol. 192, 446, 1948.
6. Semenov, V. and A. Kryazhev, "Multipactor suppression in amplitude modulated radio frequency fields," *Phys. Plasmas*, Vol. 8, 5034, 2001.
7. Rozario, N., H. F. Lenzing, F. Reardon, M. S. Zarro, and C. G. Baran, "Investigation of Telstar 4 spacecraft Ku-band and C-band antenna component for multipaction breakdown," *IEEE Trans. Microwave Theory Tech.*, Vol. 42, 558, 1994.
8. Geisser, K. H. and D. Wolk, *Proceedings of the Second International Workshop on Multipactor, RF and DC Corona and Passive Intermodulation in Space RF Hardware*, ESTEC, Noordwijk, 1996.
9. Sazontov, A., N. Vdovicheva, M. Buyanova, V. Semenov, D. Anderson, J. Puech, M. Lisak, and L. Lapierre, *Proceedings of the Fourth International Workshop on Multipactor, RF and DC Corona and Passive Intermodulation in Space RF Hardware*, ESTEC, Noordwijk, 2003.
10. Anza, S., C. Vicente, B. Gimeno, V. E. Boria, and J. Armendáriz, "Long-term multipactor discharge in multicarrier systems," *Phys. Plasmas*, Vol. 14, 082112, 2007.
11. Anza, S., M. Mattes, C. Vicente, J. Gil, D. Raboso, V. E. Boria, and B. Gimeno, "Multipactor theory for multicarrier signals," *Phys. Plasmas*, Vol. 18, 032105, 2011.
12. Anza, S., C. Vicente, J. Gil, V. E. Boria, B. Gimeno, and D. Raboso, "Nonstationary statistical theory for multipactor," *Phys. Plasmas*, Vol. 17, 062110, 2010.

13. Bouchaud, J. and A. Georges, "Anomalous diffusion in disordered media: Statistical mechanisms, models and physical applications," *Physics Reports*, Vol. 195, 127–293, 1990.

14. Edwards, A. M., et al., "Revisiting Lévy flight search patterns of wandering albatrosses, bumblebees and deer," *Nature*, Vol. 449, 1044–1049, 2007.

15. Humphries, N., et al., "Environmental context explains Lévy and Brownian movement patterns of marine predators," *Nature*, Vol. 465, 1066–1069, 2010.

16. Shlesinger, M. F., J. Klafter, and G. Zumofen, "Above, below and beyond Brownian motion," *American Journal of Physics*, Vol. 67, 1253–1259, 1999.

17. Gnedenko, B. V. and A. N. Kolmogorov, *Limit Distributions for Sums of In-dependent Random Variables*, Addison-Wesley, Reading, Massachusetts, 1968.

18. Mussawisade, K., J. E. Santos, and G. M. Schutz, "Branching-annihilating random walks in one dimension: Some exact results," *J. Phys. A: Math. Gen.*, Vol. 31, 4381–4394, 1998.

19. Furman, M. A. and M. T. F. Pivi, "Probabilistic model for the simulation of secondary electron emission," *Phys. Rev. ST Accel.*, Vol. 5, 124404, 2002.